

Chlorine activation within urban or power plant plumes: Vertically resolved ClNO₂ and Cl₂ measurements from a tall tower in a polluted continental setting

Theran P. Riedel,^{1,2} Nicholas L. Wagner,^{3,4} William P. Dubé,^{3,4} Ann M. Middlebrook,⁴ Cora J. Young,⁵ Fatma Öztürk,⁶ Roya Bahreini,⁷ Trevor C. VandenBoer,⁸ Daniel E. Wolfe,⁴ Eric J. Williams,⁴ James M. Roberts,⁴ Steven S. Brown,⁴ and Joel A. Thornton^{1,2}

Received 1 April 2013; revised 3 July 2013; accepted 8 July 2013; published 15 August 2013.

[1] Nitryl chloride (ClNO₂) is a chlorine atom source and reactive nitrogen reservoir formed during the night by heterogeneous reactions of dinitrogen pentoxide on chloride-containing aerosol particles. The main factors that influence ClNO₂ production include nitrogen oxides, ozone, aerosol surface area, soluble chloride, and ambient relative humidity. Regions with strong anthropogenic activity therefore have large ClNO₂ formation potential even inland of coastal regions due to transport or local emissions of soluble chloride. As part of the Nitrogen, Aerosol Composition, and Halogens on a Tall Tower field study, we report wintertime vertically resolved ClNO₂ and molecular chlorine (Cl₂) measurements taken on a 300 m tall tower located at NOAA's Boulder Atmospheric Observatory in Weld County, CO, during February and March of 2011. Gas and particle phase measurements aboard the tower carriage allowed for a detailed description of the chemical state of the nocturnal atmosphere as a function of height. These observations show significant vertical structure in ClNO₂ and Cl₂ mixing ratios that undergo dynamic changes over the course of a night. Using these measurements, we focus on two distinct combustion plume events where ClNO₂ mixing ratios reached 600 and 1300 parts per trillion by volume, respectively, aloft of the nocturnal surface layer. We infer ClNO₂ yields from N₂O₅-aerosol reactions using both observational constraints and box modeling. The derived yields in these plumes suggest efficient ClNO₂ production compared to the campaign average, where in-plume yields range from 0.3 to 1; the campaign average yield in the boundary layer is 0.05 ± 0.15 , with substantial night-to-night and within night variability similar to previous measurements in this region.

Citation: Riedel, T. P., et al. (2013), Chlorine activation within urban or power plant plumes: Vertically resolved ClNO₂ and Cl₂ measurements from a tall tower in a polluted continental setting, *J. Geophys. Res. Atmos.*, 118, 8702–8715, doi:10.1002/jgrd.50637.

Additional supporting information may be found in the online version of this article.

¹Department of Chemistry, University of Washington, Seattle, Washington, USA.

²Department of Atmospheric Sciences, University of Washington, Seattle, Washington, USA.

³Cooperative Institute for Research in the Environmental Sciences, University of Colorado Boulder, Boulder, Colorado, USA.

⁴NOAA Earth System Research Laboratory, Boulder, Colorado, USA.

⁵Department of Chemistry, Memorial University of Newfoundland, St. John's, Newfoundland and Labrador, Canada.

⁶Environmental Engineering Department, Abant Izzet Baysal University, Bolu, Turkey.

⁷Department of Environmental Sciences, University of California, Riverside, California, USA.

⁸Department of Chemistry, University of Toronto, Toronto, Ontario, Canada.

Corresponding author: J. A. Thornton, Department of Atmospheric Sciences, University of Washington, 408 ATG Building Box 351640, Seattle, WA 98195, USA. (thornton@atmos.washington.edu)

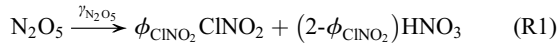
©2013. American Geophysical Union. All Rights Reserved.
2169-897X/13/10.1002/jgrd.50637

1. Introduction

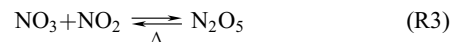
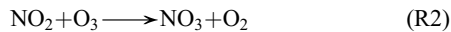
[2] Chlorine atoms have the potential to impact the oxidative environment of the troposphere due to their large reaction rate constants with most volatile organic compounds (VOC) relative to that of the hydroxyl radical (OH), the dominant tropospheric oxidant. However, both Cl atom concentrations and mechanisms for their generation have been uncertain [Knipping and Dabdub, 2003; Pszenny et al., 2007; Spicer et al., 1998]. In the boundary layer of polluted regions, two Cl atom precursors, nitryl chloride (ClNO₂) and molecular chlorine (Cl₂), have recently been quantified and shown to play a potentially important role in the evolution of oxidants and primary and secondary pollutants such as OH, O₃, and alkanes [Finley and Saltzman, 2006, 2008; Kercher et al., 2009; Lawler et al., 2011; Mielke et al., 2011; Ostroff et al., 2008; Phillips et al., 2012; Pszenny et al., 1993; Riedel et al., 2012b; Spicer et al., 1998; Thornton et al., 2010; Young et al., 2012]. However, in addition to unresolved questions related to formation mechanisms or emission sources, relatively little is known about the vertical distribution of these Cl atom precursors. To date, the

only measurements capturing the vertical distribution of ClNO_2 are limited to profiles of the Los Angeles basin urban plume by the NOAA P3 aircraft during the CalNex field study in late spring and early summer of 2010 [Young *et al.*, 2012]. Mixing ratios of ClNO_2 averaged ~ 1200 parts per trillion by volume (pptv) on individual profiles, and although there was considerable vertical variability on individual profiles, there was little vertical variability within the planetary boundary layer in an average sense. To our knowledge, there have been no vertically resolved measurements of these species in continental settings and none during wintertime when the heterogeneous chemistry of N_2O_5 , the precursor to ClNO_2 , is most important [Alexander *et al.*, 2009; Dentener and Crutzen, 1993; Tie *et al.*, 2003]. Thus, the information necessary to determine the total impact of this chlorine atom source on regional air quality remains either limited or absent.

[3] ClNO_2 is a nocturnal NO_x ($\text{NO}_2 + \text{NO}$) reservoir that photolyzes in the morning hours of the day to liberate a highly reactive chlorine atom and an NO_2 molecule. It is produced primarily at night by the reaction of dinitrogen pentoxide (N_2O_5) on chloride-containing aerosol particles [Behnke *et al.*, 1997; Bertram and Thornton, 2009; Finlayson-Pitts *et al.*, 1989; Roberts *et al.*, 2009; Thornton and Abbatt, 2005] or potentially ground surfaces [Lopez-Hilfiker *et al.*, 2012], suggesting the potential for vertical gradients to develop overnight depending upon which of these sources is most important. To our knowledge, ClNO_2 is produced only from secondary chemistry in the atmosphere and there is no evidence that ClNO_2 is directly emitted. The ClNO_2 production channel is in competition with the hydrolysis of N_2O_5 to form two HNO_3 (see R1).



[4] The yield of ClNO_2 from N_2O_5 reactions (ϕ_{ClNO_2}), which varies between 0 and 1, depends upon the particulate chloride and liquid water content; the latter of which is set by the ambient relative humidity (RH). The gross production rate of ClNO_2 also depends upon the following: (i) the NO_3 formation rate and the temperature-dependent equilibrium between N_2O_5 , NO_3 , and NO_2 (R2 and R3) [Brown *et al.*, 2009], (ii) the available aerosol surface area (SA), and (iii) the overall heterogeneous reaction probability of N_2O_5 ($\gamma_{\text{N}_2\text{O}_5}$) which in turn is a function of aerosol composition [Anttila *et al.*, 2006; Bertram and Thornton, 2009; Brown *et al.*, 2009; Folkers *et al.*, 2003; Roberts *et al.*, 2009; Thornton *et al.*, 2003].

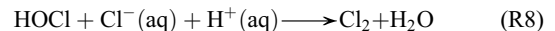
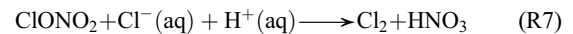
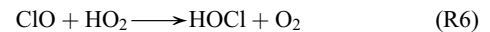
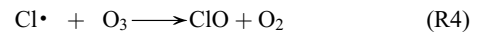


$$P_{\text{ClNO}_2} \approx \phi_{\text{ClNO}_2}(t) \gamma_{\text{N}_2\text{O}_5}(t) [\text{N}_2\text{O}_5](t) \left\{ \frac{SA(t)\omega}{4} \right\} \quad (1)$$

[5] As illustrated in equation (1), the instantaneous ClNO_2 production rate (P_{ClNO_2}) varies with time (t), both in a seasonal sense and within a night, due to the time dependences of ϕ_{ClNO_2} , $\gamma_{\text{N}_2\text{O}_5}$, N_2O_5 concentrations, SA, and aerosol composition. The bracketed portion of equation (1) describes the gas-particle collision frequency, where ω is the average molecular speed of an N_2O_5 molecule, in the free molecular regime

neglecting gas diffusion limitations. In cases where super-micron SA is significant or reaction probabilities > 0.05 , equation (1) must be modified to incorporate gas diffusion limitations.

[6] While Cl_2 has been detected in several polluted regions, albeit typically at significantly lower abundances than ClNO_2 [Finley and Saltzman, 2006, 2008; Mielke *et al.*, 2011; Riedel *et al.*, 2012b], its sources are less well understood compared to ClNO_2 . Cl_2 can be directly emitted by industrial processes like incineration and power generation [Sarwar and Bhave, 2007] but is also produced in situ via multiphase chemistry of reactive chlorine reservoirs such as ClONO_2 and HOCl [Deiber *et al.*, 2004; Gebel and Finlayson-Pitts, 2001; Vogt *et al.*, 1996]. In this mechanism, chlorine atoms react with O_3 to form ClO , which reacts with either NO_2 to form ClONO_2 or HO_2 to form HOCl (R4, R5, R6). ClONO_2 and HOCl then can react on acidic chloride-containing particles to produce Cl_2 (R7, R8), though the efficiency of these reactions in polluted urban regions is unknown [Lawler *et al.*, 2011].



[7] The Nitrogen, Aerosol Composition, and Halogens on a Tall Tower (NACHTT) study presented a unique opportunity to measure a number of the chemical species relevant to ClNO_2 and Cl_2 chemistry, allowing for the assessment of the ClNO_2 yield in a variety of air masses, the role of ground surfaces relative to aerosol particles in the formation of ClNO_2 , and the relative importance of chemical versus emission sources of Cl_2 in a continental setting. This field study represents the most complete vertical measurements of ClNO_2 and Cl_2 in the nocturnal planetary boundary layer to date. We focus much of our analysis here on two representative NO_x -rich plumes; one of which exhibited the deepest vertical extent of enhanced ClNO_2 while the other contained the highest ClNO_2 mixing ratio of the campaign. One plume is likely a more distributed combustion NO_x source such as motor vehicle traffic and other urban emissions, while the other plume is representative of a large NO_x point source such as that from a nearby power plant. Although we cannot conclusively identify the sources of either from measurements at a fixed sampling location, their vertical distributions and inferred transport times (see below) are most consistent with these assignments. We compare and contrast ClNO_2 yields, N_2O_5 -aerosol reaction probabilities, and Cl_2 within these plumes while also providing summary information on the typical characteristics that gave rise to ClNO_2 and Cl_2 at this site.

2. Methods

[8] Nitrogen, Aerosol Composition, and Halogens on a Tall Tower (NACHTT) was a collaborative research effort that took place in February and March of 2011. Its aim was to assess a number of atmospheric chemical processes

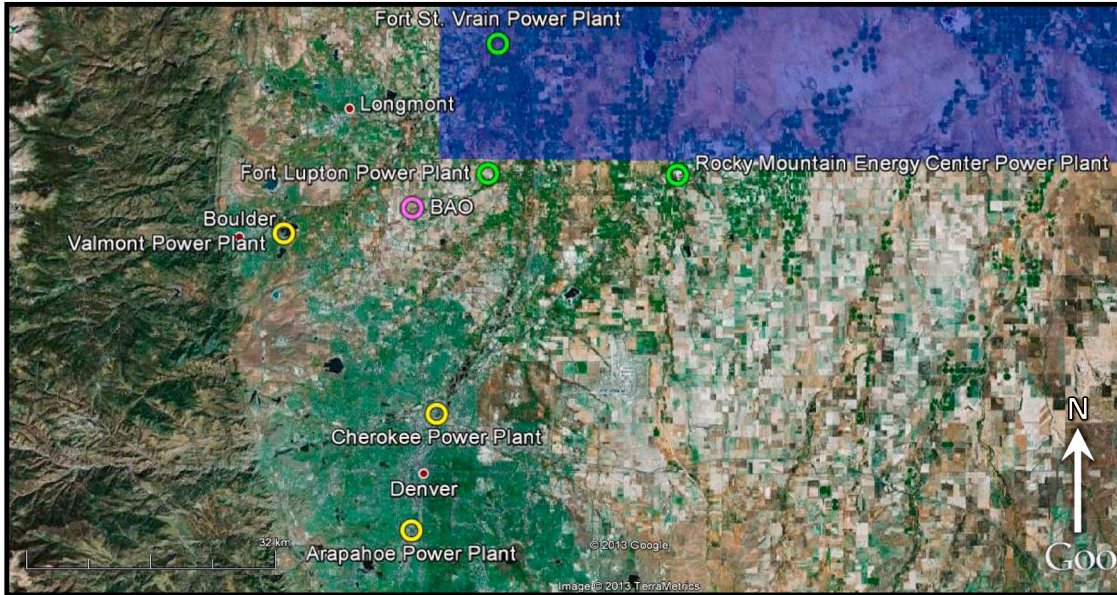


Figure 1. A map of important emission landmarks in the region surrounding the NACHTT measurement site. The measurement site is shown as an open pink circle. Small red dots illustrate the location of major cities, open yellow circles are coal-fired power plants, and open green circles are natural gas power plants. The blue-shaded region represents areas with heavy natural gas and other hydrocarbon extraction activity.

including halogen precursor chemistry in the Denver, CO, urban area [Brown *et al.*, 2013]. The measurement site (40.05° , -105.004°) was located at NOAA's Boulder Atmospheric Observatory (BAO—<http://www.esrl.noaa.gov/psd/technology/bao>) in Weld County, CO, which is about 35 km due north of the Denver urban core (see Figure 1). In addition to emissions from the Denver area which are encountered frequently, the site is also a receptor for emissions from nearby Boulder, CO, to the west, and natural gas power plant and oil and gas extraction activities to the northeast. Large local point sources of NO_x , CO_2 , SO_2 , and other primary pollutants include the Valmont coal and natural gas power plant 17 km west-southwest of the site, the Cherokee coal power plant 27 km south of the site, and the Arapahoe coal power plant 40 km south of the site (Figure 1). Commerce City, an area with oil-refining operations, is also approximately 27 km south, adjacent to the Cherokee coal power plant. Air largely unaffected by urban emissions is also routinely encountered at the site with downslope flow out of the Rocky Mountains to the west.

[9] A unique feature of this study was the incorporation of BAO's 300 m tall tower to provide vertical measurements of a number of gas phase species (HCl , HONO , HNO_3 , HNCO , organic acids, NO_x , O_3 , NO_3 , N_2O_5 , CINO_2 , Cl_2 , CO_2), particulate properties and composition (surface area, NH_4^+ , SO_4^{2-} , NO_3^- , Cl^- , organics), and meteorological data (temperature, pressure, relative humidity, wind speed, and direction). Instruments were installed in a temperature-controlled enclosure that was then mounted to the tower's payload elevator which is capable of lifting ~ 1.5 t. Instruments sampled through holes in the enclosure walls which allowed for relatively short inlets (e.g., less than 2 m for the CINO_2 instrument and substantially less than 1 m for instruments mounted near the outside wall of the enclosure), thus minimizing artifacts due to heterogeneous chemistry on inlets. The tower elevator was capable of a single

300 m vertical profile in ~ 10 min and was programmed to be controlled remotely from a nearby building. Nearly continuous vertical profiles were taken over the course of the study except in cases of high winds and snow/ice events that resulted in unsafe conditions. Fixed height measurements of meteorological and less reactive trace gases were also carried out at a number of locations on the tower, and size-resolved aerosol composition and gas-particle partitioning of several inorganic gases were measured on a 22 m scaffold mounted on a different face of the tower [Young *et al.*, 2013]. A detailed description of all the measurements taken during the NACHTT study can be found in the overview paper [Brown *et al.*, 2013].

[10] The detection scheme and the calibration setup used to obtain measurements of CINO_2 and Cl_2 are detailed in other publications [Kercher *et al.*, 2009; Riedel *et al.*, 2012b]. Briefly, all Cl^- isotopomers of CINO_2 and Cl_2 were measured at ~ 0.36 Hz by a quadrupole chemical ionization mass spectrometer (CIMS) as clusters with the iodide reagent ion, $\text{I}^-(\text{CINO}_2)^-$ and $\text{I}^-(\text{Cl}_2)^-$, respectively. A 2 m length of 6 mm inner diameter perfluoroalkoxy tubing at ambient pressure was used as the inlet line. A sampling flow rate of 1.5 standard liters per minute was maintained through the inlet to the low-pressure (~ 80 mbar) ionization region by a critical orifice and a vacuum pump. The nitrogen carrier flow through the radioactive ion source was varied by $\pm 15\%$ in order to maintain a constant pressure within the mass spectrometer as the carriage ascended and descended the tower. This variation did not appreciably alter reagent ion signals and therefore had little to no effect on instrumental sensitivity. Calibrations to both CINO_2 and Cl_2 were performed every 70 min, as in Riedel *et al.* [2012b]. Chlorine isotopic ratios matched those expected for the CINO_2 mass-to-charge ratios. A high instrumental background signal at two ($^{35}\text{Cl}^{37}\text{Cl}$ and $^{37}\text{Cl}^{37}\text{Cl}$) of the three Cl_2 cluster masses prevented similar isotopic verification for Cl_2 using the raw data. However, we approximated

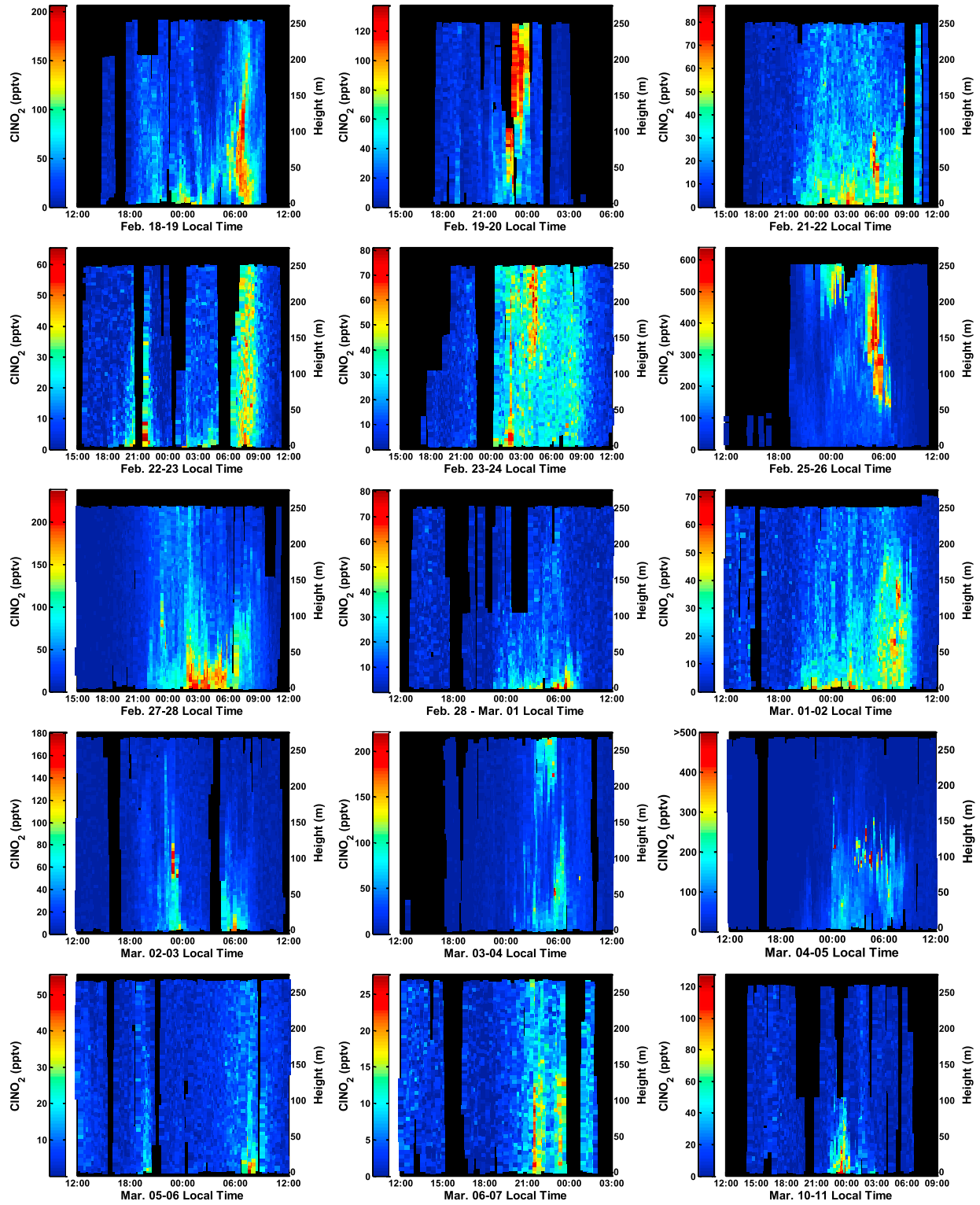


Figure 2. Fifteen day overview of NACHTT vertical ClNO_2 profiles versus time of day. Mixing ratios are shown as colored squares. Black areas indicate no available measurements. Note the color scales vary between panels.

the background interferences at each time point by using the signals present at the contaminated mass-to-charge ratios during a time period when there was no signal at the dominant Cl_2 mass ($^{35}\text{Cl}^{35}\text{Cl}$). Subtracting these background estimates from the raw data produced good agreement with the expected Cl_2 ratios

based on the natural isotope abundances. The raw data were averaged to 10 s in order to reduce the uncertainty of each datum due to counting statistics. This resulted in a reported measurement about every 10 m in altitude during a vertical profile with a measurement uncertainty of ~20%. Given the instrument duty

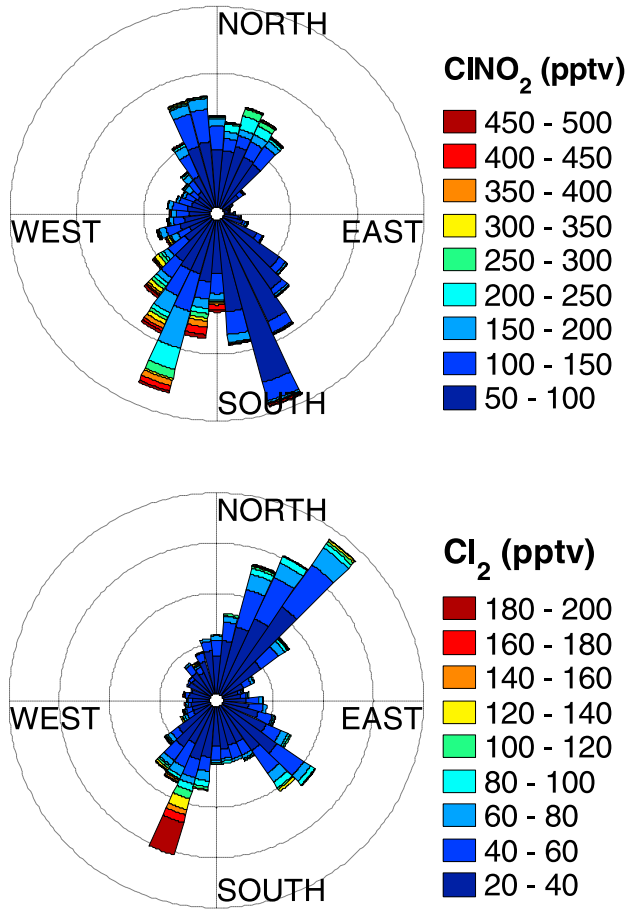


Figure 3. A wind rose showing the frequency of CINO₂ (top) and Cl₂ (bottom) observations with wind direction colored by mixing ratios for the NACHTT study.

cycles, averaging time associated with the CIMS, aerosol composition, and gas phase acid measurements, coupled with the narrow extent of certain plume observations in the vertical and in time, the number of data points available within these plumes can be few. That said, it is important to note that each data point within a plume is precise and not the result of instrumental noise. Inlet transmission tests in which ~2 parts per billion by volume (ppbv) N₂O₅ was added to the inlet while sampling ambient air were also routinely performed to ensure that CINO₂ and Cl₂ were not produced in appreciable quantities by reactions on sampling lines (CINO₂:N₂O₅ < 0.03; Cl₂:N₂O₅ < 0.02).

3. Results and Discussion

3.1. Overview of Observations

[11] Consistent with previous ground-based measurements in this region [Thornton *et al.*, 2010], CINO₂ was routinely observed at night during the entirety of NACHTT (see Figure 2) with the largest mixing ratios occurring when high RH (>50%) plumes enhanced in NO_x and depleted in O₃ were sampled. The study average nighttime maximum CINO₂ mixing ratio was 270 ± 260 pptv (1σ) with a maximum observed mixing ratio of 1300 pptv. CINO₂ mixing ratios were variable in the vertical, with some enhanced layers being less than 50 m in depth and persisting for a few minutes. In other cases CINO₂ mixing ratios were greater

than 100 pptv from tens of meters above ground level, extending to and likely beyond the highest point reached by the tower carriage (265 m). Such plumes were also persistent, observed at the measurement site for hours at a time. There does not appear to be one single factor which can explain the night-to-night variability or variability with height in a given night. The most import factors appear to be polluted air from the surrounding urban areas or large combustion sources, relative humidity (RH) greater than 40%, and time since sunset (see Supporting Information Figures S1–S5). CINO₂ was almost always positively associated with RH and exhibited a local enhancement near ground level where the temperatures were colder and the RH higher. The lowest CINO₂ levels were often observed at higher altitudes when RH was below 40%. Figure 2 shows 15 days' worth of vertically resolved CINO₂ observations during which vertical profiles were continuously taken for >3 h. Overall, there was typically CINO₂ near the surface (~60 pptv nightly maxima) possibly arising from N₂O₅ deposition to the ground or reaction on aerosol particles, the liquid water content of which in these low altitude, high RH conditions potentially enhance CINO₂ production through a higher N₂O₅ reaction probability [Behnke *et al.*, 1997; Bertram and Thornton, 2009; Raff *et al.*, 2009; Thornton *et al.*, 2003]. Importantly, the largest CINO₂ values (>200 pptv) of the study were typically aloft and associated with plumes that were markedly separate from the CINO₂ that appeared associated with the surface layer. Moreover, based on the wind direction at the time of sampling, these plumes are most likely associated with urban and power plant sources. As shown in Figure 3, major CINO₂ events were generally localized to two directions relative to the measurement site, south or southwest wind flow (Denver-Boulder urban corridor) and occasionally during north or northeast winds (natural gas extraction fields).

[12] Cl₂ was always less abundant than CINO₂ (see Supporting Information Figure S6) with a study average nighttime mixing ratio within the instrumental error of zero (~2 pptv). On a few occasions, enhanced Cl₂ was detected at night; similar to CINO₂, Cl₂ observations most often occurred when winds were from specific sectors (south southwest, southeast, and north northeast—see Figure 3). The maximum observed mixing ratio of 320 pptv, as with all observations greater than 100 pptv, was limited to a few time periods and confined to a few tens of meters in the vertical, consistent with a specific point source. These Cl₂ plumes tended to also be high in NO_x and CO₂, potentially indicating emission from nearby power plants and/or associated cooling towers, or other chlorine emitting processes such as waste disposal or incineration [Chang and Allen, 2006; Raff *et al.*, 2009; Sarwar and Bhave, 2007].

[13] In what follows, we focus on two specific plume intercepts, one that occurred in the early morning of 26 February and the other that occurred in the early morning of 5 March. For simplicity, we refer to the plume encountered on 26 February as plume 1 and the plume encountered on 5 March as plume 2. These plumes are subsets of the two classes of air masses which contained elevated CINO₂ or Cl₂, i.e., the broadly polluted urban region and specific combustion point sources.

3.2. Plume 1: Diffuse Urban Pollution

[14] The vertical distribution of CINO₂ and Cl₂ mixing ratios observed in plume 1 are shown in Figure 4. The plume is

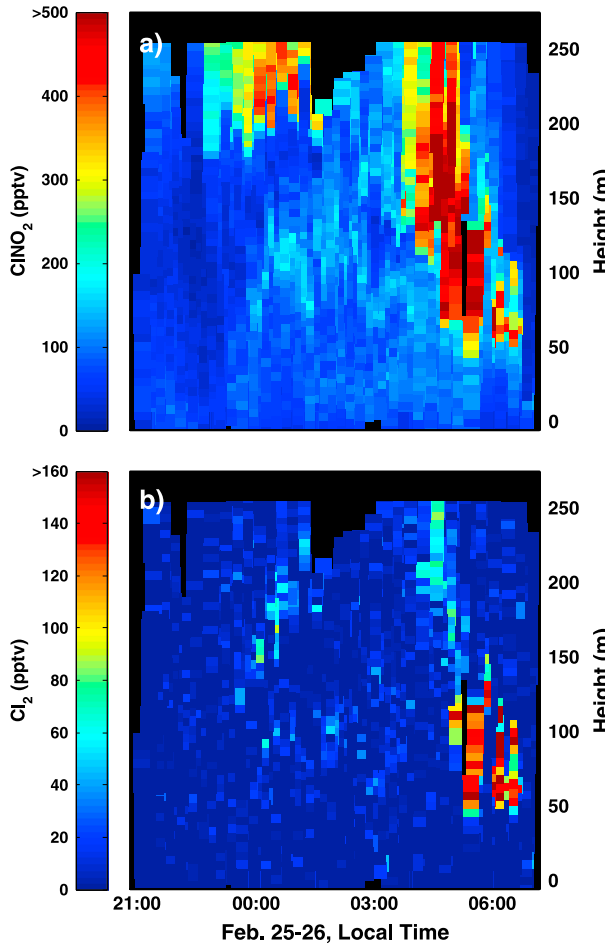


Figure 4. Vertical profiles versus time of day for (a) ClNO₂ and (b) Cl₂ mixing ratios during the time period around plume 1. Mixing ratios are shown as colored squares; the color scale for ClNO₂ saturates at 500 pptv, while that for Cl₂ saturates at 160 pptv. Black areas indicate no available measurements.

first intercepted around 3:00 A.M. local time and is continuously sampled for approximately 3.5 h until sunrise at ~6:30 A.M. The ClNO₂ color scale in Figure 4a saturates at 500 pptv. Plume 1 represents some of the highest sustained ClNO₂ observed during the campaign with an average mixing ratio of 340 ± 120 pptv (1σ) and a maximum value of 640 pptv. It was a relatively deep plume, with depths spanning between 75 m and greater than 150 m and elevated mixing ratios appear to extend beyond the measurement ceiling. During the first 1.5 h that the plume was sampled, the ClNO₂ layer was deep (>100 m) and consistently sampled. At ~5:00 A.M., the depth of the ClNO₂ plume decreases and Cl₂ becomes enhanced to ~140 pptv possibly representing a change in the plume chemistry, the source of the plume, or a mixing of sources. Average Cl₂ mixing ratios in the plume were 30 ± 40 pptv (1σ) with a maximum of 190 pptv. The Cl₂ color scale in Figure 4b saturates at 160 pptv.

[15] Figure 5 illustrates the vertical structure of ClNO₂, Cl₂, N₂O₅, aerosol chloride, aerosol nitrate, HNO₃, CO₂, NO₂, O₃, potential temperature (θ), and RH during one of the plume 1 transects that occurred between 4:36 A.M. and 4:44 A.M. Lower mixing ratios of ClNO₂ near 100 pptv are

present over the first 60 m above the surface. This portion of the average profile had a particularly high RH (>90%) and is representative of the persistent near-surface ClNO₂ formation observed throughout the campaign. N₂O₅ is low over the first 60 m, either due to titration by fresh NO emissions or to efficient uptake onto aerosols and ground surfaces at high RH [Chang et al., 2011]. Above 60 m, plume 1 becomes apparent with large increases in ClNO₂ and N₂O₅ that persist to the top of the profile. Cl₂ is also elevated within this transect at heights >150 m, with mixing ratios of a few tens of pptv. Aerosol nitrate is largest near the surface (~5 ppbv) and decreases sharply to ~2.5 ppbv at the bottom of the plume, remaining relatively constant until 175 m where it decreases steadily. There is no marked enhancement in aerosol chloride, HNO₃, CO₂, NO₂, or O₃ within the plume, and NO₂ and O₃ are strongly anticorrelated (slope = -0.50, R = -0.95). The RH only falls below 50% during the top 10 m of the profile, between 240 and 250 m above ground level. Potential temperature gradually increases with height throughout the profile, with steep increases between 50 and 60 m, and again above 180 m. These inversions represent separations between individual layers and are coincident with the changes in the chemical composition described above. The largest ClNO₂ observations during this profile occurred when the winds were from 158° (south southeast) relative to the measurement site. In general this corresponds to winds coming from the Denver urban area south of the site. The same was true for maximum Cl₂ observations, indicating a correlation in the source region for these two species.

3.3. Plume 2: Combustion Point Source

[16] The largest ClNO₂ mixing ratio of the NACHTT study occurred on 5 March. For the purpose of comparison, we apply a similar description of the plume that contained this observation (referred to as plume 2) as for plume 1. Multiple ClNO₂ and Cl₂ vertical profiles taken during the plume 2 intercept are shown in Figure 6. Plume 2 is likely first sampled at ~3:00 A.M. and is sampled intermittently until ~4:00 A.M. Compared to plume 1, plume 2 is significantly narrower in depth. ClNO₂ enhancements were largely confined to heights between 80 and 120 m, and the enhancements had distinctly sharp edges. The maximum ClNO₂ mixing ratio detected in these intercepts was 1300 pptv, though this maximum was not observed on every transect shown in Figure 6, possibly due to meandering of the plume away from and toward the tower, or time-dependent changes in plume composition or chemistry. The color scale in Figure 6a saturates at 500 pptv. Plume 2 had a Cl₂ average mixing ratio of 3 ± 20 pptv (1σ) with a maximum of 120 pptv. As with Figure 4b, shortly prior to sunrise at ~6:30 A.M., there is a slight increase in Cl₂ mixing ratios to values near 50 pptv. However, at this point, it is likely that plume 2 is no longer being sampled, given the stark changes in the ClNO₂ and Cl₂ vertical profiles.

[17] As stated above, plume 2 represents a particularly confined plume in terms of ClNO₂ and Cl₂. This is apparent in Figure 7 which shows ClNO₂, Cl₂, N₂O₅, aerosol chloride, aerosol nitrate, HNO₃, CO₂, NO₂, O₃, potential temperature, and RH for the vertical profile that contained the 1300 pptv ClNO₂ observation (4:12 A.M.–4:21 A.M.). The sharpness of the plume in terms of ClNO₂ and Cl₂ between 75 and 110 m, together with coincident enhancements in aerosol

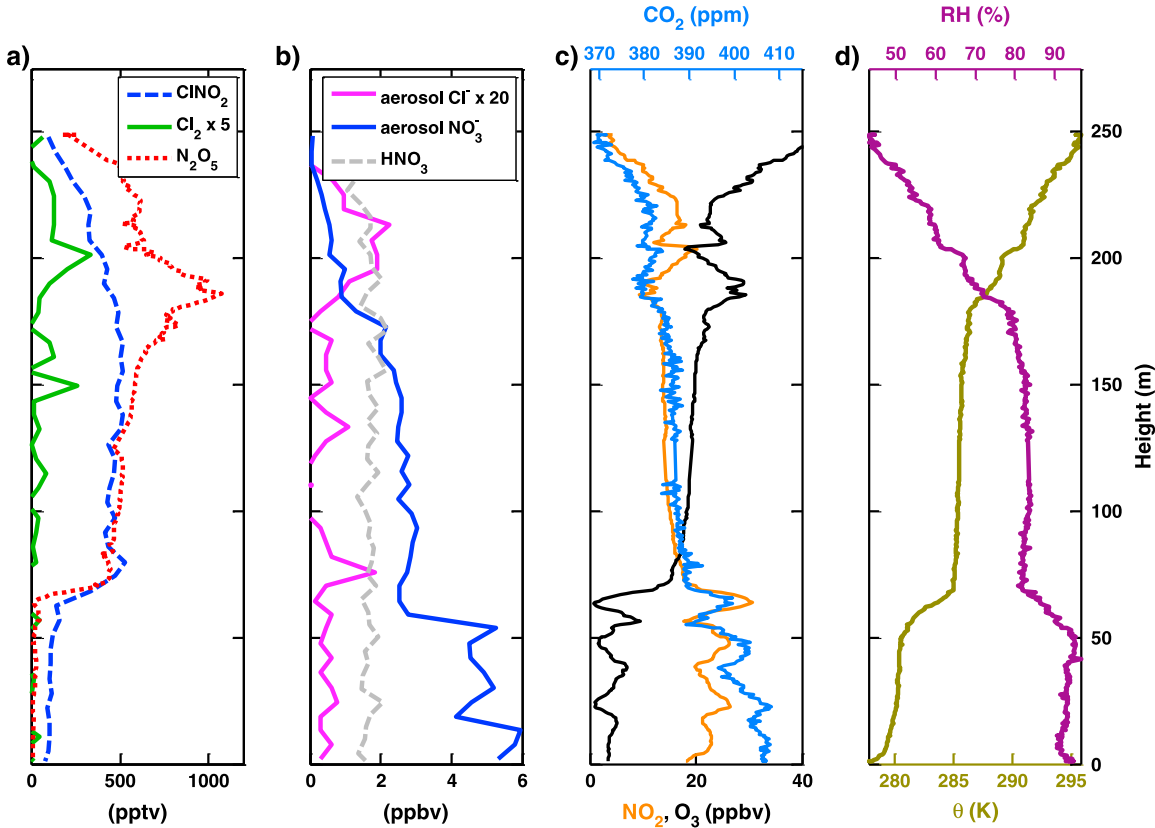


Figure 5. Observations taken during a plume 1 intercept. (a) CINO₂ (blue dashed line), Cl₂ × 5 (green solid line), and N₂O₅ (red dotted line) mixing ratios. (b) Aerosol phase Cl⁻ × 20 (pink solid line) and NO₃⁻ (blue solid line), gas phase HNO₃ (grey dashed line). (c) CO₂ (cyan solid line, top x axis), NO₂ (orange solid line, bottom x axis), and O₃ (black solid line, bottom x axis) mixing ratios. (d) Relative humidity (RH (%), purple solid line) and potential temperature (θ (K), olive solid line).

chloride, CO₂, and NO₂ indicates that it likely originated from a local point source, possibly from one of the power plants indicated earlier (see section 2). Aloft of this enhanced CINO₂ layer, RH drops steeply and θ increases with height. N₂O₅ remains sustained while NO₂ and O₃ decrease above this layer likely due to a smaller reaction probability on aerosols at low RH. The apparent decoupling of CINO₂ and N₂O₅ just above the enhanced CINO₂ layer suggests that the components and/or environmental conditions necessary for CINO₂ production were not fully coincident with NO_x in the vertical. The aerosol chloride measurement (Figure 7b) supports this argument, illustrating that particle phase chloride was present only in the CINO₂ layer. In general, aerosol chloride showed enrichments during preceding plume 2 intercepts (see Supporting Information Figure S11) that had CINO₂ mixing ratios in excess of 200 pptv and showed similar vertical trends, indicating the plume source emitted significant amount of chloride in addition to the CINO₂ precursor compounds. Additionally, the uptake of N₂O₅ on aerosol particles above the enhanced CINO₂ layer could be inefficient, given the low RH (<40%) which could account for some of the decoupling. The majority of CINO₂ and Cl₂ observations during the intercepts of plume 2 occurred when the winds were out of the southwest at 226°. Given this general direction, the point source is likely one of the coal-fired combustion sources such as the Arapahoe, Cherokee, or Valmont power plants (see Figure 1).

3.4. CINO₂ Yield Estimates

[18] We use several different approaches to infer CINO₂ yields from the observations. Each of these approaches requires assumptions, either due to the Eulerian sampling framework or the incomplete measurement suite. We therefore refrain from reporting specific yield values and instead give a range of likely yields based on the combined results of all approaches.

[19] Following the work of Wagner *et al.* [2012], we use the vertically resolved observations of total nitrate (aerosol phase NO₃⁻ + gas phase HNO₃) and CINO₂ taken during the plume intercepts to derive an observation-based estimate of the CINO₂ yield from reactions of N₂O₅ in the two plumes. Based on the relationship introduced in reaction R1, in a nocturnal air mass evolving in time, CINO₂ will be linearly related to the total amount of NO₃⁻ in the gas and particle phase produced by N₂O₅ reactions as shown below in equation (2).

$$m = \frac{\Delta \text{CINO}_2}{\Delta \text{NO}_3^-} = \frac{\phi_{\text{CINO}_2}}{2 - \phi_{\text{CINO}_2}} \quad (2)$$

$$\phi_{\text{CINO}_2} = \frac{2m}{1+m} \quad (3)$$

[20] The slope m of a regression line fitted to a scatter plot of CINO₂ versus total NO₃⁻ is then related to the molar

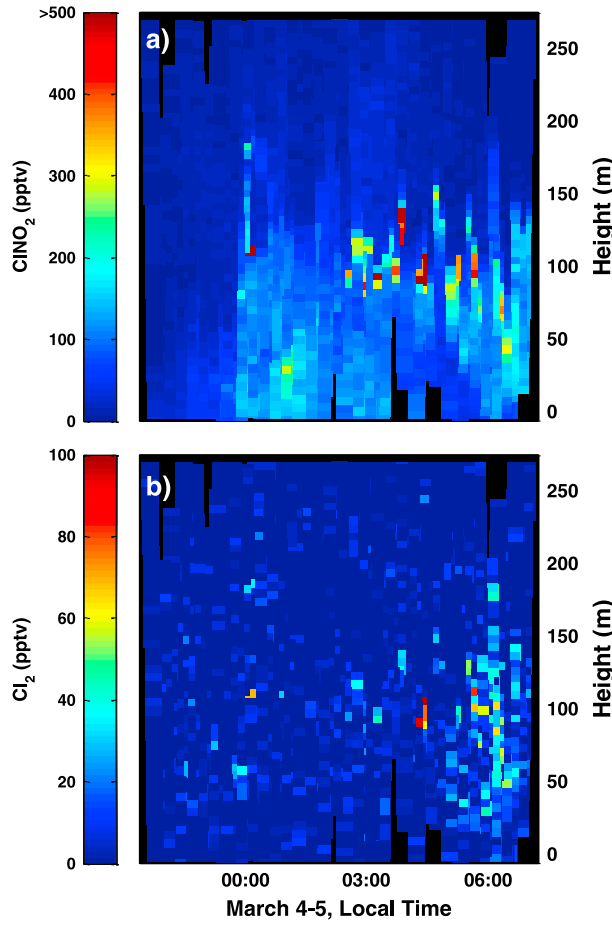


Figure 6. Vertical profiles versus time of day for (a) ClNO_2 and (b) Cl_2 mixing ratios during the time period around plume 2. Mixing ratios are shown as colored squares; the color scale for ClNO_2 saturates at 500 pptv, while that for Cl_2 saturates at 100 pptv. Black areas indicate no available measurements.

yield of ClNO_2 per mole of N_2O_5 reacted, equation (3), subject to several assumptions. First, we neglect the production of HNO_3 or organic nitrates from NO_3^- reactions with hydrocarbons due to the much colder temperatures and high NO_x conditions, which favors N_2O_5 over NO_3^- (R3), when ClNO_2 was typically observed during NACHTT. Particulate NO_3^- has a sufficiently long lifetime that its concentration can be influenced by the previous day's photochemistry or even by NO_3^- production from the previous night. These effects likely bias our yield estimates low. Additionally, this approach assumes a constant N_2O_5 reaction probability and a constant ClNO_2 yield since the origin of the plume. In reality these quantities are unlikely to remain constant over the plume lifetime and the apparent correlations may in fact represent variable chemical histories containing emissions from multiple sources of different ages and initial conditions that therefore could potentially result in variable intercepts and slopes. Changes in temperature and RH as well as the buildup of nitrate due to plume processing and the consumption of chloride to form ClNO_2 have the potential to further alter these quantities. However, given the data available, these assumptions are a necessary simplification in order to obtain estimates of said parameters, but as a result, these estimates are more representative of values

averaged over the lifetime of the plume up to the time it was sampled as opposed to an instantaneous estimate.

[21] In Figure 8 we show the nighttime relationship of ClNO_2 to total NO_3^- at different heights measured over the course of the study. Lines corresponding to ϕ_{ClNO_2} of 0.05, 0.15, 0.4, and 1.0 are drawn for illustrative purposes only given the caveats discussed above. In general, the figure demonstrates robustly that ClNO_2 and total NO_3^- measured at night were positively correlated ($R = 0.35$), with the slope and intercept varying significantly with height and from night-to-night as we show in Figure 8. The overall relationship in Figure 8 shows two populations: low elevations generally exhibiting a low yield (shallow slope), possibly due to the presence of daytime nitrate, and higher elevations exhibiting a comparatively higher yield (steeper slope). Vertical structure in the gas phase HNO_3 measurement was not as pronounced as that for aerosol phase NO_3^- ; as such, most of the variation in the nitrate is driven by particulate nitrate. Though precautions were taken to avoid any time delays as a result of inlet effects, such as the use of a heated inlet, the reduced vertical structure may have resulted from the time response of the inlet for the HNO_3 instrument [see, e.g., Fehsenfeld *et al.*, 1998]. Details regarding the HNO_3 measurement can be found elsewhere (T. C. VandenBoer, Understanding the role of the ground surface in HONO vertical structure: High-resolution vertical profiles during NACHTT-11, submitted to *Journal of Geophysical Research: Atmospheres*, 2013). However, reduced time response in HNO_3 is not expected to significantly bias the estimates considering that gas phase HNO_3 was largely constant with respect to a single profile.

[22] Based on these relationships, we estimate that the typical ϕ_{ClNO_2} aloft in this region during wintertime is 0.05 ± 0.15 , consistent with box modeling of observations made from a nearby ground-based site [Thornton *et al.*, 2010]. In order to obtain this estimate, we only select data taken at heights >75 m with NO_2 values larger than 8 ppbv thereby removing surface effects and selecting data representative of urban conditions aloft. In general ϕ_{ClNO_2} for the surface layer is likely well below that for the air aloft considering the large total nitrate values and modest ClNO_2 levels measured near the surface.

[23] We also apply this same ClNO_2 versus total NO_3^- approach to the individual transects of plumes 1 and 2 discussed above. As shown in Figure 9a, these estimates give $\phi_{\text{ClNO}_2} \approx 0.3$ and $\phi_{\text{ClNO}_2} \approx 0.7$ for plume 1 and plume 2, respectively. Data below 100 m are omitted from the calculation of the estimated plume 1 yield shown in Figure 9a (left pane), and similarly, data below 85 m are omitted from the plume 2 yield estimate shown in Figure 9a (right pane). This precaution is taken to ensure effects of the ground surface do not influence these strictly in-plume estimates. As we outlined in section 2, the narrow extent of plume 2 in the vertical (<25 m in depth) and in time (ClNO_2 mixing ratios >500 pptv are only encountered during two successive vertical profiles), allow for few data points within the plume. That said, a similar ϕ_{ClNO_2} was obtained from another transect of the plume that took place 6 min prior to that described in Figure 9a (see Supporting Information Figure S14). Apart from this additional transect, it is unlikely we sampled the plume during any of the other vertical profiles as the major characteristics defining plume 2 ($\text{ClNO}_2 > 500$ pptv and elevated Cl_2) were not found in other profiles.

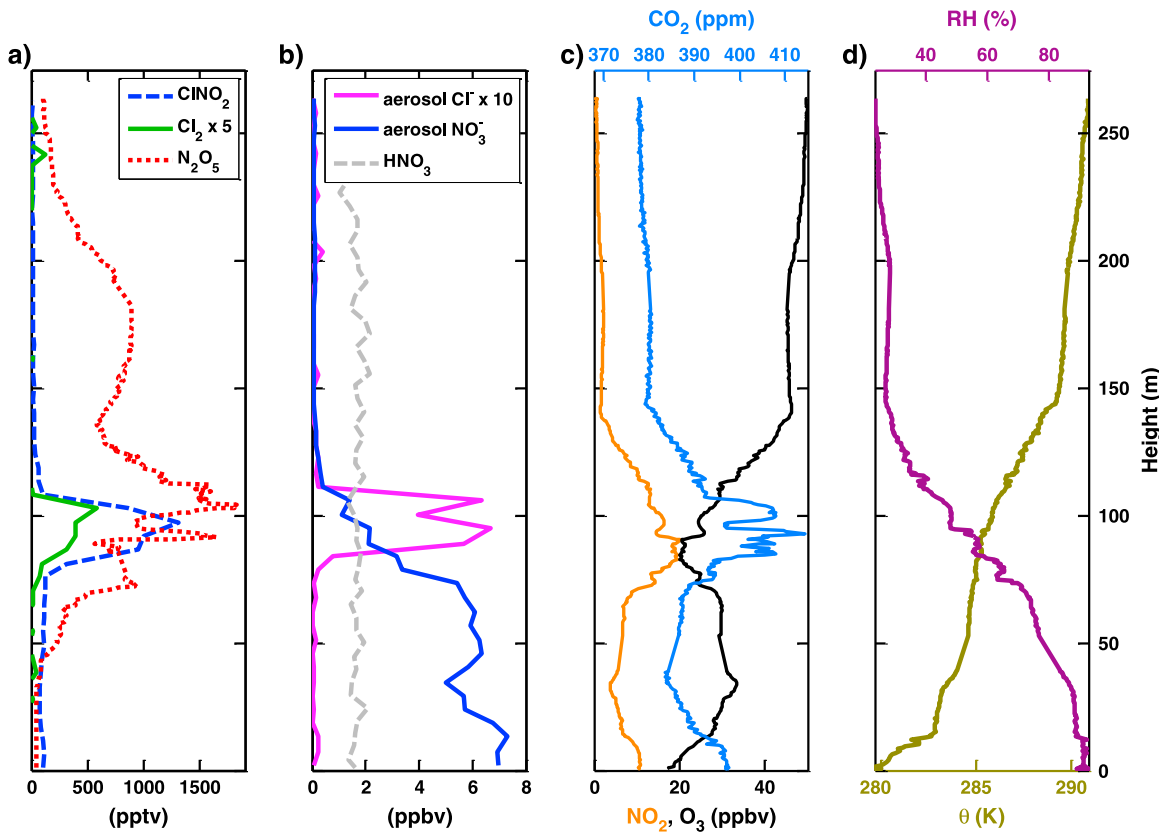


Figure 7. Observations taken during a plume 2 intercept. (a) ClNO_2 (blue dashed line), $\text{Cl}_2 \times 5$ (green solid line), and N_2O_5 (red dotted line) mixing ratios. (b) Aerosol phase $\text{Cl}^- \times 10$ (pink solid line) and NO_3^- (blue solid line), gas phase HNO_3 (grey dashed line). (c) CO_2 (cyan solid line, top x axis), NO_2 (orange solid line, bottom x axis), and O_3 (black solid line, bottom x axis) mixing ratios. (d) Relative humidity (RH (%), purple solid line) and potential temperature (θ K), olive solid line).

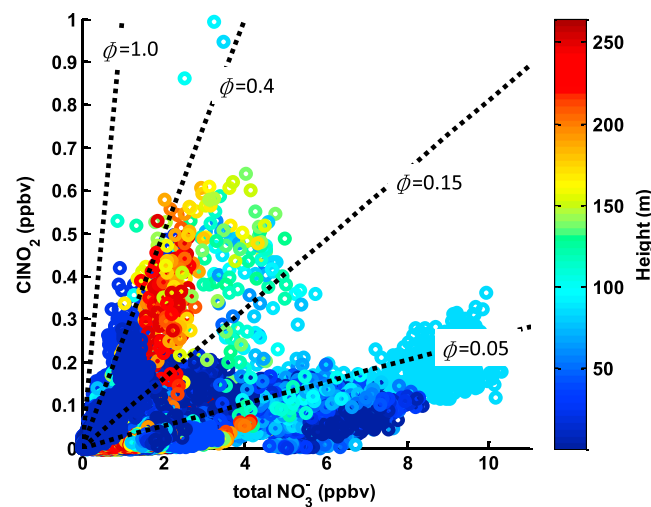


Figure 8. ClNO_2 mixing ratios are plotted versus total nitrate ($\text{HNO}_3(\text{g}) + \text{aerosol phase } \text{NO}_3^-$) mixing ratios illustrating the positive relationship between the two species that varied significantly with height over the course of the study. Each point is colored by the height at which the measurement was taken. Lines corresponding to various approximate ClNO_2 yields, based on equation (2), are drawn through the origin for illustrative purposes only.

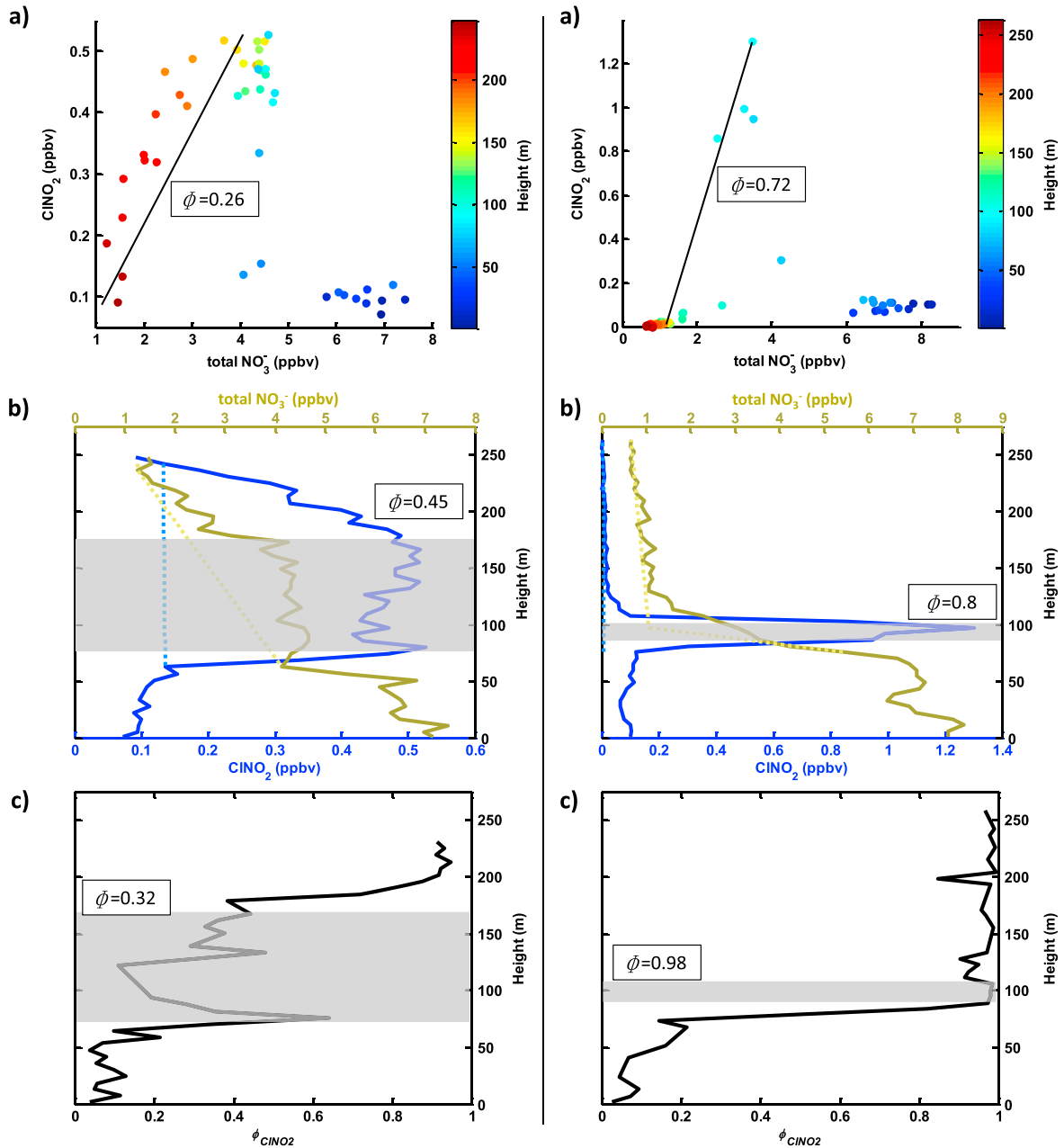


Figure 9. Summary of CINO_2 yield estimate approaches for plume 1 (left pane) and plume 2 (right pane). (a) CINO_2 mixing ratios are plotted versus total nitrate ($\text{HNO}_3(g) + \text{aerosol phase } \text{NO}_3^-$) mixing ratios for the single transect. Each point is colored by the height at which the measurement was taken. The slope of the solid black lines, which are least squares linear fits to data in the plumes (data below 100 m are omitted from the plume 1 fit; data below 85 m are omitted from the plume 2 fit), together with equation (3), are used to estimate the in-plume CINO_2 yield shown next to the line. (b) Vertical profile of CINO_2 mixing ratios and total nitrate mixing ratios. In estimating the given CINO_2 yield for the plume, the dotted lines are used as background values to determine the in-plume (shaded region) enhancements of CINO_2 and total nitrate. (c) Height versus estimated CINO_2 yields obtained from aerosol composition data and aerosol thermodynamic modeling. The stated yield represents the average of the yields over the shaded region.

[24] A related but alternative approach to infer a CINO_2 yield is to determine the enhancements of both CINO_2 and total NO_3^- within distinct plumes relative to the values outside of the plumes. As illustrated in Figure 9b, we use the enhancements of CINO_2 and total NO_3^- in plumes 1 and 2 as estimates of ΔCINO_2 and ΔNO_3^- in equation (2). The enhancements are determined by subtracting the background-mixing ratios from the

plume center defined by the maxima in CINO_2 over the profile. Background-mixing ratios of CINO_2 and NO_3^- are determined by linear interpolations of data outside the plume (low in CINO_2) which occur above and below the plume center as shown by the dotted lines in Figure 9b. This background interpolation, while uncertain, is necessary to remove enhancements in NO_3^- which are apparently unrelated to the

Table 1. Summary of Box Modeling Constraints and Results

	Plume 1: 26 February	Plume 2: 5 March
Target O ₃ (ppbv)	16.2	24.5
Target NO ₂ (ppbv)	17	16.4
Target N ₂ O ₅ (ppbv)	0.4335	0.907
Target ClNO ₂ (ppbv)	0.527	1.3
Aerosol surface area ($\mu\text{m}^2\text{cm}^{-3}$)	264	130
Modeled time (hours)	3.3	4.4
Initial O ₃ (ppbv)	48	49
Initial NO (ppbv)	20	22
ϕ_{ClNO_2} (constrained)	0.38	0.85
$\gamma_{\text{N}_2\text{O}_5}$	0.024	0.02
Time since sunset (hours)	10.7	10.3
Initial O ₃ (ppbv)	69	64
Initial NO (ppbv)	35	31
ϕ_{ClNO_2}	0.06	0.19
$\gamma_{\text{N}_2\text{O}_5}$	0.022	0.023

plumes and are possibly residual NO₃⁻ from photochemical production the day before. Large preexisting nitrate values if left completely unaccounted for would artificially drive the estimated ClNO₂ yields to low values. Calculating the relative enhancement of ClNO₂ to NO₃⁻ in the plumes (denoted by the grey-shaded areas) gives ϕ_{ClNO_2} for plumes 1 and 2 as 0.45 and 0.8, respectively. These values do not change significantly if a constant NO₃⁻ background, defined only by the high altitude NO₃⁻ values, is used instead of the interpolated values. This constant background approach assumes that any NO₃⁻ above the background at lower altitudes is the result of a nighttime NO₃⁻ source. The resulting ϕ_{ClNO_2} values for both plumes are similar to the other two approaches: 0.4 and 0.7 for plumes 1 and 2, respectively.

[25] In a third approach, we utilize the aerosol composition measurements provided by an aerosol mass spectrometer (AMS) mounted in the tower carriage to derive an estimate of ϕ_{ClNO_2} . Using the Extended AIM (Aerosol Inorganics Model) thermodynamic aerosol model (available at <http://www.aim.env.uea.ac.uk/aim/aim.php>) and the measured RH and aerosol composition (shown for plumes 1 and 2 in Supporting Information Figure S15), we can obtain an estimate of the amount of particulate water present [Clegg *et al.*, 1998]. Given this estimate of aerosol water concentration and the measured aerosol chloride concentration, ϕ_{ClNO_2} can be estimated using equation (4) which is based on a number of laboratory studies estimating the relative rates of ClNO₂ versus HNO₃ formation from N₂O₅ heterogeneous reactions [Behnke *et al.*, 1997; Bertram and Thornton, 2009; Roberts *et al.*, 2009]. The uncertainty associated with this approach arises mainly from the aerosol chloride measurement, only nonrefractory chloride is efficiently measured by the AMS, and the effect of the organic aerosol fraction on particulate water calculated by the thermodynamic aerosol model. We assume the organic species do not contribute to the water content of the aerosols. Moreover, these calculations represent instantaneous yields that assume all the chloride is available for reaction with N₂O₅ and do not account for depletion of chloride or mixing and transport prior to the measurement. The results of this approach for plumes 1 and 2 are shown in Figure 9c with estimated yields for plumes 1 and 2 of 0.32 and 0.98, respectively. Again, the grey-shaded regions are used to determine these in-plume yields.

$$\phi_{\text{ClNO}_2} \approx \frac{1}{1 + \frac{[\text{H}_2\text{O}]}{450[\text{Cl}^-]}} \quad (4)$$

[26] Results from the multiple ϕ_{ClNO_2} estimate approaches described above indicate the $\phi_{\text{ClNO}_2} \approx 0.3\text{--}0.45$ and $\phi_{\text{ClNO}_2} \approx 0.7\text{--}1$ for plumes 1 and 2, respectively. It is important to note that these yields are not representative of the entire vertical extent of the plume but only for the conditions that give rise to the largest (>500 pptv) ClNO₂ values. That said, these ϕ_{ClNO_2} are similar to those found in polluted coastal regions and suggest that ClNO₂ production can be efficient within inland combustion plumes such as those associated with power generation. The plume 1 yield is of similar magnitude to the largest yield inferred from previous wintertime measurements in Denver/Boulder area [Thornton *et al.*, 2010]. The estimated yield for plume 2 indicates efficient ClNO₂ production comparable to what would be expected in polluted marine environments, though confined to a very narrow vertical extent.

3.5. Plume Box Modeling

[27] That plumes 1 and 2 are well isolated from the ground surface and likely experience little nighttime vertical mixing represents conditions well suited for box model applications where the reactions are assumed to proceed in a static volume. We use a 0-D time-dependent chemical box model to further investigate the nocturnal chemical processing within the two plumes that lead to these largest ClNO₂ values of the study. A goal with this modeling is to determine whether the observations can be simulated using the above estimates of ϕ_{ClNO_2} and reasonable estimates of $\gamma_{\text{N}_2\text{O}_5}$ and plume age. Gas phase reaction rate constants in the model are taken from the most recent data available on the International Union of Pure and Applied Chemistry kinetics database (<http://www.iupac-kinetic.ch.cam.ac.uk>). The model is given initial inputs of NO, O₃, aerosol surface area, temperature, and pressure, which are chosen so the model output matches observations taken during the two plume intercepts. The initial conditions are thus indicative of the chemical conditions at or near the emission source. We assume all NO_x is initially emitted as NO, which is subsequently oxidized by O₃ to NO₂, and that $\gamma_{\text{N}_2\text{O}_5}$ and ϕ_{ClNO_2} remain constant over the lifetime of the plume. Due to the cold plume temperatures (~0°C), the equilibrium between N₂O₅, NO₃, and NO₂ (R3) is strongly shifted toward N₂O₅ (N₂O₅:NO₃ ~ 250:1 for typical plume NO₂ values). In addition, given the low abundance of biogenic VOC and other NO₃ sinks, we assume that N₂O₅ losses dominate over that of NO₃. The NO₃ lifetime in the model is arbitrarily set to 30 min. Model outputs are fairly insensitive to this assumption. For example, adjusting the NO₃ lifetime by a factor of 10 in either direction changes modeled N₂O₅ and ClNO₂ mixing ratios by less than 7%. The ϕ_{ClNO_2} is fixed to the yields calculated in section 3.4, while $\gamma_{\text{N}_2\text{O}_5}$ and the reaction time (plume age) are adjustable parameters that are varied to best match the observations of O₃, NO₂, N₂O₅, ClNO₂, and the NO₃⁻ enhancements shown in the plumes. A complete table of the reactions and rates used in the box model can be found in the supporting information (Table S1).

[28] A summary of the modeling results are shown in Table 1. The resulting $\gamma_{\text{N}_2\text{O}_5}$ is similar for both plumes at ~0.02 which falls within the range (<0.001–0.1) of $\gamma_{\text{N}_2\text{O}_5}$

reported from laboratory studies on a variety of different particle types and for different temperatures; these values are comparable to larger observations of $\gamma_{\text{N}_2\text{O}_5}$ obtained from direct measurements on ambient particles, though those measurements were not taken during wintertime [Bertram et al., 2009; Hallquist et al., 2003; Hu and Abbatt, 1997; Mozurkewich and Calvert, 1988; Riedel et al., 2012a]. The $\gamma_{\text{N}_2\text{O}_5}$ estimates are also of similar magnitude to those predicted by an iterative box model analysis that predicts $\gamma_{\text{N}_2\text{O}_5}$ using all of the observations taken during NACHTT [Wagner et al., 2013]. For the select data used in that analysis, the distribution in $\gamma_{\text{N}_2\text{O}_5}$ was centered near 0.018. Given the moderate to high ϕ_{ClNO_2} estimated for the two plumes, these results are also conceptually consistent with our understanding of N_2O_5 heterogeneous chemistry in that similar factors have been shown to influence both $\gamma_{\text{N}_2\text{O}_5}$ and ϕ_{ClNO_2} [Bertram and Thornton, 2009; Riedel et al., 2012a; Roberts et al., 2009]. While these estimates do place useful constraints on $\gamma_{\text{N}_2\text{O}_5}$ and ϕ_{ClNO_2} , the most robust constraint is the product of the two quantities because both can vary relative to each other to produce the same amount of ClNO_2 (see equation (1)).

[29] The resulting time required by the model to best match the observations is an indication of plume age. In both cases, this age is significantly less than the time since sunset. For plume 1, an age of ~ 4 h is reasonable, considering an ideal case in which the air within the plume is transported directly to the measurement site from central Denver with the same wind speed observed at the measurement site. This results in a processing time of ~ 4 h. Similarly, in the case of plume 2, given the wind speed and approximate direction within the plume, the transit time from the Valmont power plant to the site is estimated to be at least 2 h and the transit time from the Arapahoe power plant to the site is ~ 4 h. An alternative option for the reaction/processing time is to run the model as if the plume originated at sunset which is also shown in Table 1. However, using the constraints on ϕ_{ClNO_2} and the NO_3^- enhancements in the plumes, we were unable to match the observations, supporting the conclusion that these plumes were emitted well after sunset. Disregarding these constraints and using the time since sunset as the reaction time results in $\phi_{\text{ClNO}_2} = 0.06$ and $\gamma_{\text{N}_2\text{O}_5} = 0.022$ for plume 1 and $\phi_{\text{ClNO}_2} = 0.19$ and $\gamma_{\text{N}_2\text{O}_5} = 0.023$ for plume 2. Because the time since sunset is the maximum possible reaction time, these ϕ_{ClNO_2} values can be considered lower limits for the two plumes.

[30] The uncertainty in plume age contributes uncertainty in the model predictions. Brown et al. [2006] use observations of O_3 and NO_2 to approximate the age of nocturnal plumes. There is clearly a negative relationship between O_3 and NO_2 in plumes 1 and 2, which is consistent with nocturnal emission and/or processing, and in a Lagrangian sense that slope can be equated to age. However, the variations with height of the O_3 versus NO_2 slope suggest wind shear or mixing effects on the O_3 and NO_2 relationship. Variations in time and space such as fresh injections into existing plumes and mixing complicate an age estimate based on this relationship. The clear dependences on height and time shown for the two plumes suggest that, while persistent ClNO_2 production can occur throughout the plume volume like plume 1, there may well be a set of distinct NO_x sources and injection heights with varying ages within a sampling period and vertical region.

[31] NACHTT represents only the third time that ClNO_2 and Cl_2 have been measured simultaneously and presents an opportunity to investigate the proposed conversion of ClNO_2 to Cl_2 via heterogeneous chemistry [Mielke et al., 2011; Riedel et al., 2012b; Roberts et al., 2008]. Using the model, we add a heterogeneous loss of ClNO_2 to form Cl_2 with unit yield and adjust the corresponding aerosol reaction probability for ClNO_2 to reproduce the observed Cl_2 mixing ratios. The resulting aerosol reaction probability for ClNO_2 conversion to Cl_2 is 0.001, or less, for the two plume cases which is about 6 times lower than that given in Roberts et al. [2008] for acidic aerosols ($\text{pH} < 2$). Observationally constrained estimates of aerosol pH were made during NACHTT at 9 m [Young et al., 2013]. While not directly comparable to the altitudes of plumes 1 and 2, these estimates suggest $\text{pH} > 3$, consistent with the low conversion rate of ClNO_2 to Cl_2 we infer from the model. Given that the enhanced Cl_2 occurred only when sampling from a specific sector and that aerosol pH was likely > 3 , we conclude it was more likely that the observed Cl_2 was coemitted with ClNO_2 precursors rather than produced by ClNO_2 heterogeneous chemistry.

[32] Finally, we can use the box model to assess the maximum possible ClNO_2 production in plumes similar to those we characterized above. Assuming emission at sunset and chemical evolution over the entire night (~ 13 h) based on the model parameters and constraints derived above, we estimate the maximum possible ClNO_2 produced could reach 2.5 to 4 ppbv. This estimate assumes a vertically static reaction volume. The previous, limited available data on plume transport at night suggest that mixing may be quite limited [Brown et al., 2012]. The largest ClNO_2 values could be well downwind of the emission location by some 50–100 km, and past the NACHTT measurement location, with larger effects on the chemistry in these regions than inferred from our observations described in this paper.

4. Conclusions

[33] Over the course of the study, ClNO_2 and Cl_2 were observed on most nights. Similar to measurements off the coast of Los Angeles, we conclude that Cl_2 is more likely the result of direct emissions rather than conversion from ClNO_2 , which is produced only from N_2O_5 heterogeneous chemistry. Though the nocturnal atmosphere at this site was highly stratified, as expected for a wintertime continental setting, mixing ratios of both species approached those reported in the polluted marine boundary layer where the large chloride source from sea salt aerosol is more obvious than inland sources. All air masses enhanced in ClNO_2 were characterized by moderate to high RH (45–90%) and originated from the urban areas of Denver and the Front Range of the Rocky Mountains, as well as from regions with significant natural gas extraction activities. Enhanced Cl_2 mixing ratios were measured when air originated from a much narrower section of the Denver metro area.

[34] Using the expected nocturnal relationship between ClNO_2 and total NO_3^- and the measured aerosol composition, we inferred a variable yield of ClNO_2 from N_2O_5 chemistry that spanned nearly the entire allowable range (0–1). The exact causes of this variability remain uncertain but likely involve, in part, the availability of aerosol chloride driven either by particle phase (low yields at low RH) or by partitioning of the chloride into a portion of the aerosol population with a

smaller fraction of the available surface area. ClNO_2 production was most efficient within the plume of a combustion point source which we attribute to a local power plant. This finding raises the possibility that power generation is at least part of the widespread ClNO_2 production inferred by Thornton *et al.* [2010]. Coal-burning and water-cooling operations associated with power generation are recognized but uncertain sources of soluble chloride. Our measurements are strongly suggestive that the nocturnal processing of power plants plumes leads to ClNO_2 formation. Aircraft and modeling studies are needed to confirm this result and determine the implications for regional air quality and NO_x processing.

[35] **Acknowledgments.** This work was supported by a grant from the National Science Foundation (NSF CAREER ATM-0846183 to J.A.T.). T.P.R. is grateful for an Earth System Science graduate fellowship from the National Aeronautics and Space Administration (NASA NESSF NNX10AN48H). We also thank Charles Brock for providing aerosol surface area measurements.

References

- Alexander, B., M. G. Hastings, D. J. Allman, J. Dachs, J. A. Thornton, and S. A. Kunasek (2009), Quantifying atmospheric nitrate formation pathways based on a global model of the oxygen isotopic composition ($\Delta^{17}\text{O}$) of atmospheric nitrate, *Atmos. Chem. Phys.*, 9(14), 5,043–5,056, doi:10.5194/acp-9-5043-2009.
- Anttila, T., A. Kiendler-Scharr, R. Tillmann, and T. F. Mentel (2006), On the reactive uptake of gaseous compounds by organic-coated aqueous aerosols: Theoretical analysis and application to the heterogeneous hydrolysis of N_2O_5 , *J. Phys. Chem. A*, 110(35), 10,435–10,443, doi:10.1021/jp062403c.
- Behnke, W., C. George, V. Scheer, and C. Zetzsch (1997), Production and decay of ClNO_2 , from the reaction of gaseous N_2O_5 with NaCl solution: Bulk and aerosol experiments, *J. Geophys. Res.*, 102(D3), 3,795–3,804, doi:10.1029/96JD03057.
- Bertram, T. H., and J. A. Thornton (2009), Toward a general parameterization of N_2O_5 reactivity on aqueous particles: The competing effects of particle liquid water, nitrate and chloride, *Atmos. Chem. Phys.*, 9(21), 8,351–8,363, doi:10.5194/acp-9-8351-2009.
- Bertram, T. H., J. A. Thornton, T. P. Riedel, A. M. Middlebrook, R. Bahreini, T. S. Bates, P. K. Quinn, and D. J. Coffman (2009), Direct observations of N_2O_5 reactivity on ambient aerosol particles, *Geophys. Res. Lett.*, 36, L19803, doi:10.1029/2009GL040248.
- Brown, S. S., et al. (2009), Reactive uptake coefficients for N_2O_5 determined from aircraft measurements during the Second Texas Air Quality Study: Comparison to current model parameterizations, *J. Geophys. Res.*, 114, D00F10, doi:10.1029/2008JD011679.
- Brown, S. S., et al. (2012), Effects of NO_x control and plume mixing on nighttime chemical processing of plumes from coal-fired power plants, *J. Geophys. Res.*, 117, D07304, doi:10.1029/2011JD016954.
- Brown, S. S., et al. (2006), Nocturnal odd-oxygen budget and its implications for ozone loss in the lower troposphere, *Geophys. Res. Lett.*, 33, L08801, doi:10.1029/2006GL025900.
- Brown, S. S., et al. (2013), Nitrogen, Aerosol Composition and Halogens on a Tall Tower (NACHTT): Overview of a wintertime air chemistry field study in the front range urban corridor of Colorado, *J. Geophys. Res. Atmos.*, 118, doi:10.1002/jgrd.50537.
- Chang, S. Y., and D. T. Allen (2006), Atmospheric chlorine chemistry in southeast Texas: Impacts on ozone formation and control, *Environ. Sci. Technol.*, 40(1), 251–262, doi:10.1021/es050787z.
- Chang, W. L., P. V. Bhave, S. S. Brown, N. Riener, J. Stutz, and D. Dabdub (2011), Heterogeneous atmospheric chemistry, ambient measurements, and model calculations of N_2O_5 : A review, *Aerosol Sci. Tech.*, 45(6), 665–695, doi:10.1080/02786826.2010.551672.
- Clegg, S. L., P. Brimblecombe, and A. S. Wexler (1998), Thermodynamic model of the system $\text{H}^+ - \text{NH}_4^+ - \text{Na}^+ - \text{SO}_4^{2-} - \text{NO}_3^- - \text{Cl}^- - \text{H}_2\text{O}$ at 298.15 K, *J. Phys. Chem. A*, 102(12), 2,155–2,171, doi:10.1021/jp973043j.
- Deiber, G., C. George, S. Le Calve, F. Schweitzer, and P. Mirabel (2004), Uptake study of ClONO_2 and BrONO_2 by Halide containing droplets, *Atmos. Chem. Phys.*, 4, 1,291–1,299, doi:10.5194/acp-4-1291-2004.
- Dentener, F. J., and P. J. Crutzen (1993), Reaction of N_2O_5 on tropospheric aerosols: Impact on the global distributions of NO_x , O_3 , AND OH, *J. Geophys. Res.*, 98(D4), 7,149–7,163, doi:10.1029/92JD02979.
- Fehsenfeld, F. C., L. G. Huey, D. T. Sueper, R. B. Norton, E. J. Williams, F. L. Eisele, R. L. Mauldin, and D. J. Tanner (1998), Ground-based intercomparison of nitric acid measurement techniques, *J. Geophys. Res.*, 103(D3), 3,343–3,353, doi:10.1029/97JD02213.
- Finlayson-Pitts, B. J., M. J. Ezell, and J. N. Pitts (1989), Formation of chemically active chlorine compounds by reactions of atmospheric NaCl particles with gaseous N_2O_5 and ClONO_2 , *Nature*, 337(6204), 241–244, doi:10.1038/337241a0.
- Finley, B. D., and E. S. Saltzman (2006), Measurement of Cl_2 in coastal urban air, *Geophys. Res. Lett.*, 33, L11809, doi:10.1029/2006GL025799.
- Finley, B. D., and E. S. Saltzman (2008), Observations of Cl_2 , Br_2 , and I_2 in coastal marine air, *J. Geophys. Res.*, 113, D21301, doi:10.1029/2008JD010269.
- Folkers, M., T. F. Mentel, and A. Wahner (2003), Influence of an organic coating on the reactivity of aqueous aerosols probed by the heterogeneous hydrolysis of N_2O_5 , *Geophys. Res. Lett.*, 30(12), 1644, doi:10.1029/2003GL017168.
- Gebel, M. E., and B. J. Finlayson-Pitts (2001), Uptake and reaction of ClONO_2 on NaCl and synthetic sea salt, *J. Phys. Chem. A*, 105(21), 5,178–5,187, doi:10.1021/jp0046290.
- Hallquist, M., D. J. Stewart, S. K. Stephenson, and R. A. Cox (2003), Hydrolysis of N_2O_5 on sub-micron sulfate aerosols, *Phys. Chem. Chem. Phys.*, 5(16), 3,453–3,463, doi:10.1039/b301827j.
- Hu, J. H., and J. P. D. Abbatt (1997), Reaction probabilities for N_2O_5 hydrolysis on sulfuric acid and ammonium sulfate aerosols at room temperature, *J. Phys. Chem. A*, 101(5), 871–878, doi:10.1021/jp9627436.
- Kercher, J. P., T. P. Riedel, and J. A. Thornton (2009), Chlorine activation by N_2O_5 : Simultaneous, in situ detection of ClNO_2 and N_2O_5 by chemical ionization mass spectrometry, *Atmos. Meas. Tech.*, 2(1), 193–204, doi:10.5194/amt-2-193-2009.
- Knipping, E. M., and D. Dabdub (2003), Impact of chlorine emissions from sea-salt aerosol on coastal urban ozone, *Environ. Sci. Technol.*, 37(2), 275–284, doi:10.1021/es025793z.
- Lawler, M. J., R. Sander, L. J. Carpenter, J. D. Lee, R. von Glasow, R. Sommariva, and E. S. Saltzman (2011), HOCl and Cl_2 observations in marine air, *Atmos. Chem. Phys.*, 11(15), 7,617–7,628, doi:10.5194/acp-11-7617-2011.
- Lopez-Hilfiker, F. D., K. Constantin, J. P. Kercher, and J. A. Thornton (2012), Temperature dependent halogen activation by N_2O_5 reactions on halide-doped ice surfaces, *Atmos. Chem. Phys.*, 12(11), 5,237–5,247, doi:10.5194/acp-12-5237-2012.
- Mielke, L. H., A. Furgeson, and H. D. Osthoff (2011), Observation of ClNO_2 in a mid-continent urban environment, *Environ. Sci. Technol.*, 45(20), 8,889–8,896, doi:10.1021/es201955u.
- Mozurkewich, M., and J. G. Calvert (1988), Reaction probability of N_2O_5 on aqueous aerosols, *J. Geophys. Res.*, 93(D12), 15,889–15,896, doi:10.1029/JD093D12p15889.
- Osthoff, H. D., et al. (2008), High levels of nitryl chloride in the polluted subtropical marine boundary layer, *Nat. Geosci.*, 1(5), 324–328, doi:10.1038/ngeo177.
- Phillips, G. J., M. J. Tang, J. Thieser, B. Brickwedde, G. Schuster, B. Bohn, J. Lelieveld, and J. N. Crowley (2012), Significant concentrations of nitryl chloride observed in rural continental Europe associated with the influence of sea salt chloride and anthropogenic emissions, *Geophys. Res. Lett.*, 39, L10811, doi:10.1029/2012GL051912.
- Pszenny, A. A. P., E. V. Fischer, R. S. Russo, B. C. Sive, and R. K. Varner (2007), Estimates of Cl atom concentrations and hydrocarbon kinetic reactivity in surface air at Appledore Island, Maine (USA), during International Consortium for Atmospheric Research on Transport and Transformation/Chemistry of Halogens at the Isles of Shoals, *J. Geophys. Res.*, 112, D10S13, doi:10.1029/2006JD007725.
- Pszenny, A. A. P., W. C. Keene, D. J. Jacob, S. Fan, J. R. Maben, M. P. Zetwo, M. Springer-Young, and J. N. Galloway (1993), Evidence of inorganic chlorine gases other than hydrogen chloride in marine surface air, *Geophys. Res. Lett.*, 20(8), 699–702, doi:10.1029/93GL00047.
- Raff, J. D., B. Njegic, W. L. Chang, M. S. Gordon, D. Dabdub, R. B. Gerber, and B. J. Finlayson-Pitts (2009), Chlorine activation indoors and outdoors via surface-mediated reactions of nitrogen oxides with hydrogen chloride, *Proc. Natl. Acad. Sci. U. S. A.*, 106(33), 13,647–13,654, doi:10.1073/pnas.0904195106.
- Reff, A., P. V. Bhave, H. Simon, T. G. Pace, G. A. Pouliot, J. D. Mobley, and M. Houyoux (2009), Emissions inventory of PM2.5 trace elements across the United States, *Environ. Sci. Technol.*, 43(15), 5,790–5,796, doi:10.1021/es082930x.
- Riedel, T. P., T. H. Bertram, O. S. Ryder, S. Liu, D. A. Day, L. M. Russell, C. J. Gaston, K. A. Prather, and J. A. Thornton (2012a), Direct N_2O_5 reactivity measurements at a polluted coastal site, *Atmos. Chem. Phys.*, 12(6), 2,959–2,968, doi:10.5194/acp-12-2959-2012.
- Riedel, T. P., et al. (2012b), Nitrily chloride and molecular chlorine in the coastal marine boundary layer, *Environ. Sci. Technol.*, 46(19), 10,463–10,470, doi:10.1021/es204632r.
- Roberts, J. M., H. D. Osthoff, S. S. Brown, and A. R. Ravishankara (2008), N_2O_5 oxidizes chloride to Cl_2 in acidic atmospheric aerosol, *Science*, 321(5892), 1,059–1,059, doi:10.1126/science.1158777.

- Roberts, J. M., H. D. Osthoff, S. S. Brown, A. R. Ravishankara, D. Coffman, P. Quinn, and T. Bates (2009), Laboratory studies of products of N_2O_5 uptake on Cl^- containing substrates, *Geophys. Res. Lett.*, 36, L20808, doi:10.1029/2009GL040448.
- Sarwar, G., and P. V. Bhave (2007), Modeling the effect of chlorine emissions on ozone levels over the eastern United States, *J. Appl. Meteorol. Climatol.*, 46(7), 1,009–1,019, doi:10.1175/jam2519.1.
- Spicer, C. W., E. G. Chapman, B. J. Finlayson-Pitts, R. A. Plastridge, J. M. Hubbe, J. D. Fast, and C. M. Berkowitz (1998), Unexpectedly high concentrations of molecular chlorine in coastal air, *Nature*, 394(6691), 353–356, doi:10.1038/28584.
- Thornton, J. A., and J. P. D. Abbatt (2005), N_2O_5 reaction on submicron sea salt aerosol: Kinetics, products, and the effect of surface active organics, *J. Phys. Chem. A*, 109(44), 10,004–10,012, doi:10.1021/jp054183t.
- Thornton, J. A., C. F. Braban, and J. P. D. Abbatt (2003), N_2O_5 hydrolysis on sub-micron organic aerosols: The effect of relative humidity, particle phase, and particle size, *Phys. Chem. Chem. Phys.*, 5(20), 4,593–4,603, doi:10.1039/b307498f.
- Thornton, J. A., et al. (2010), A large atomic chlorine source inferred from mid-continent reactive nitrogen chemistry, *Nature*, 464(7286), 271–274, doi:10.1038/nature08905.
- Tie, X. X., et al. (2003), Effect of sulfate aerosol on tropospheric NO_x and ozone budgets: Model simulations and TOPSE evidence, *J. Geophys. Res.*, 108(D4), 8364, doi:10.1029/2001JD001508.
- Vogt, R., P. J. Crutzen, and R. Sander (1996), A mechanism for halogen release from sea-salt aerosol in the remote marine boundary layer, *Nature*, 383(6598), 327–330, doi:10.1038/383327a0.
- Wagner, N. L., et al. (2012), The sea breeze/land breeze circulation in Los Angeles and its influence on nitryl chloride production in this region, *J. Geophys. Res.*, 117, D00V24, doi:10.1029/2012JD017810.
- Wagner, N. L., et al. (2013), N_2O_5 uptake coefficients and nocturnal NO_2 removal rates determined from ambient wintertime measurements, *J. Geophys. Res. Atmos.*, 118, doi:10.1002/jgrd.50653.
- Young, C. J., et al. (2012), Vertically resolved measurements of nighttime radical reservoirs in Los Angeles and their contribution to the urban radical budget, *Environ. Sci. Technol.*, 46(20), 10,965–10,973, doi:10.1021/es302206a.
- Young, A. H., W. C. Keene, A. A. P. Pszenny, R. Sander, J. A. Thornton, T. P. Riedel, and J. R. Maben (2013), Phase partitioning of soluble trace gases with size-resolved aerosols in near-surface continental air over northern Colorado, USA during winter, *J. Geophys. Res. Atmos.*, 118, doi:10.1002/jgrd.50653.